

Statefinder Parameters for Interacting Phantom Energy with Dark Matter

Baorong Chang*, Hongya Liu†, Lixin Xu, Chengwu Zhang and Yongli Ping

School of Physics & Optoelectronic Technology, Dalian University of Technology, Dalian, 116024, P. R. China

We apply in this paper the statefinder parameters to the interacting phantom energy with dark matter. There are two kinds of scaling solutions in this model. It is found that the evolving trajectories of these two scaling solutions in the statefinder parameter plane are quite different, and that are also different from the statefinder diagnostic of other dark energy models.

PACS numbers: 98.80.-k, 98.80.Es

Cosmic observations indicate that our universe is undergoing an accelerated expansion and the dominated component of the present universe is dark energy [1, 2, 3, 4, 5]. The Wilkinson Microwave Anisotropy Probe (WMAP) satellite experiment tells us that dark energy, dark matter, and the usual baryonic matter occupy about 73%, 23%, and 4% of the total energy of the universe, respectively. The accelerated expansion of the present universe is attributed to the dark energy whose essence is quite unusual and there is no justification for assuming that it resembles known forms of matter or energy. Candidates for dark energy have been widely studied and focus on the cosmological constant Λ [6, 7] with $\mathcal{W} = -1$, a dynamically evolving scalar field (quintessence) [8, 9] with $\mathcal{W} > -1$ and phantom [10] with $\mathcal{W} < -1$. Recently, a study of high- \mathcal{Z} (\mathcal{Z} is redshift) SNe Ia [11] find that the equation of state of dark energy has a 99% probability of being $\mathcal{W} < -1$ if no priors are placed on Ω_m^0 . When these SNe results are combined with CMB and 2dFGRS the 95% confidence limits on an unevolving equation of state are $-1.46 < \mathcal{W} < -0.78$ [3, 11] which is consistent with estimates made by other groups [4, 5]. In order to obtain $\mathcal{W} < -1$, phantom field with reverse sign in its dynamical term may be a simplest way and can be regarded as one of interesting possibilities describing dark energy [12]. However, the other physical properties of phantom energy are rather weird, as they include violation of the dominant-energy condition, naive superluminal sound speed and increasing energy density with time. The latter property ultimately leads to unwanted future singularity called big rip which had been considered in [13]. This singularity is characterized by the divergence of the scale factor in a finite time in future [14].

Many authors have discussed various kinds of phantom field models to avoid the cosmic doomsday [15], which require a special class of phantom field potentials with a local maximum. Moreover, the energy density of the phantom field increases with time, while the energy density of the matter fluid decreases as the universe expands. Why are the energy density of dark matter and the phantom energy density of the same order just at the present epoch? This coincidence problem becomes more difficult to solve in the phantom model without the suitable interaction [16]. But Guo et al. in Ref. [17, 18] proposed a suitable interaction in the phantom field model, and the coincidence problem can be avoided. Moreover in Ref. [18], the universe also avoids the big rip. In Ref. [18], considering a universe model which contains phantom field ϕ and the dark matter ρ_{dm} . The Friedmann equation in a spatially flat FRW metric can be written as follows:

$$H^2 = \frac{\kappa^2}{3}(\rho_\phi + \rho_{dm}), \quad (1)$$

and

$$\dot{H} = -\frac{\kappa^2}{2}(\rho_{dm} - \dot{\phi}^2), \quad (2)$$

where $\kappa^2 \equiv 8\pi G$, ρ_{dm} is the energy density of the dark matter, and the dark matter possesses the equation of state $P_{dm} = 0$. The energy density and pressure of the phantom field ϕ are ρ_ϕ and P_ϕ , respectively,

$$\rho_\phi = -\frac{1}{2}\dot{\phi}^2 + V(\phi), \quad (3)$$

$$P_\phi = -\frac{1}{2}\dot{\phi}^2 - V(\phi). \quad (4)$$

* changbaorong@student.dlut.edu.cn

† Corresponding author: hylu@dlut.edu.cn

where $V(\phi)$ is the phantom field potential, $V(\phi) = V_0 \exp(-\lambda\kappa\phi)$. Here, we postulate that the two component ρ_ϕ and ρ_{dm} , interact through the interaction term Q according to

$$\dot{\rho}_\phi + 3H(\rho_\phi + P_\phi) = -Q, \quad (5)$$

$$\dot{\rho}_{dm} + 3H(\rho_{dm} + P_{dm}) = Q. \quad (6)$$

Here, the interaction term has the specific formation

$$Q = 3cH(\rho_\phi + \rho_{dm}). \quad (7)$$

where c is a dimensionless parameter denoting the transfer strength. We define the following dimensionless variables

$$x = \frac{\kappa\dot{\phi}}{\sqrt{6}H}, \quad y = \frac{\kappa\sqrt{V}}{\sqrt{3}H}, \quad z = \frac{\kappa\sqrt{\rho_{dm}}}{\sqrt{3}H}. \quad (8)$$

Thus the fractional densities of ρ_ϕ and ρ_{dm} are

$$\Omega_\phi = -x^2 + y^2, \quad \Omega_{dm} = z^2. \quad (9)$$

The evolution equations (5) and (6) can be written as the following set of equations:

$$x' = -3x(1 + x^2 - \frac{1}{2}z^2 - \frac{1}{2}cx^{-2}) - \frac{\sqrt{6}}{2}\lambda y^2, \quad (10)$$

$$y' = -3y(x^2 + \frac{\sqrt{6}}{6}\lambda x - \frac{1}{2}z^2), \quad (11)$$

$$z' = -3z(\frac{1}{2} + x^2 - \frac{1}{2}z^2 - \frac{1}{2}cz^{-2}), \quad (12)$$

where the prime denotes a derivative with respect to the logarithm of the scale factor, $N = \ln a$. From the definitions of these new variables, we find that the equation of state of phantom \mathcal{W}_ϕ is $\mathcal{W}_\phi = (-x^2 - y^2)/(-x^2 + y^2)$. So we get the effective parameter of equation-of-state of the phantom is

$$\mathcal{W}_\phi^{eff} = \frac{-x^2 - y^2 + c}{-x^2 + y^2}. \quad (13)$$

and the effective equation of state for the total cosmic fluid is

$$\mathcal{W}_{eff} = -x^2 - y^2. \quad (14)$$

Guo et al. in Ref. [18] had concluded that in the case of the interaction (7), there exist two stable scaling solutions, the climbing-up scaling solution and the rolling-down scaling solution. In this model the universe evolves from a matter-dominated phase to a scaling solution, which is characterized by a constant ratio of the energy densities of the dark matter and the phantom field, which may give a phenomenological solution of the coincidence problem. In the climbing-up case, the phantom field initially climbs up, the effective equation of state \mathcal{W}_{eff} realizes a transition from $\mathcal{W}_{eff} > -1$ to $\mathcal{W}_{eff} < -1$, and the universe ends with a big rip. In the rolling-down case, the phantom field initially rolls down, the effective equation of state tends to above -1 and realizes a transition from $\mathcal{W}_{eff} < -1$ to $\mathcal{W}_{eff} > -1$, in this case the cosmic doomsday is avoided and the universe accelerates forever. There have been so many models that proposed to explain the cosmic acceleration and solve, or at least alleviate, the coincidence problem [9, 19, 20]. In order to discriminate this interacting phantom model from others, and differentiate these two scaling solutions further, we refer to a cosmological diagnostic pair $\{r, s\}$ called statefinder which is introduced by Sahni et al. in [21] and defined as

$$r \equiv \frac{\ddot{a}}{aH^3}, \quad s \equiv \frac{r-1}{3(q-1/2)}, \quad (15)$$

Here q is the deceleration parameter. The statefinder is a "geometrical" diagnostic in the sense that it depends on the expansion factor and hence on the metric describing space-time. Since different cosmological models involving dark energy exhibit qualitatively different evolution trajectories in the $s-r$ plane, this statefinder diagnostic can differentiate various kinds of dark energy models. For the spatially flat LCDM cosmological model, the statefinder parameters

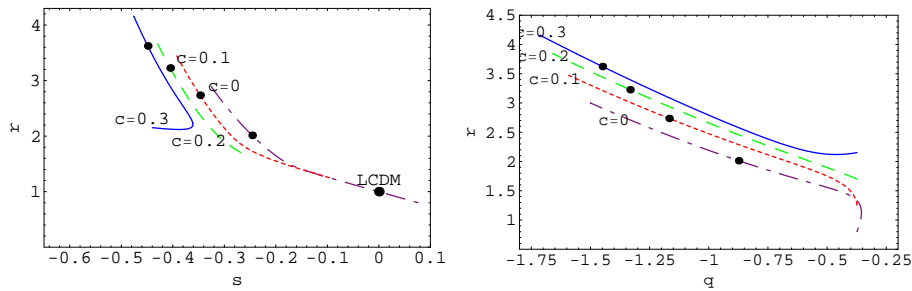


FIG. 1: The left figure is $s-r$ diagram of the climbing-up scaling solution with $x_0 < 0$. The right figure is $q-r$ diagram of the climbing-up scaling solution with $x_0 < 0$. The curves evolve in the variable interval $N \in [-2, 20]$. Selected curves for $\lambda = 1$, $c = 0, 0.1, 0.2$ and 0.3 respectively. Dots locate the current values of the statefinder parameters.

correspond to a fixed point $\{r = 1, s = 0\}$. So far, some models including the cosmological constant, quintessence, phantom, quintom, the Chaplygin gas, braneworld models, holographic models, interacting and coupling dark energy models [20, 21, 22], have been successfully differentiated. For example, the quintessence model with inverse power law potential, the phantom model with power law potential and the Chaplygin gas model all tend to approach the LCDM fixed point, but for quintessence and phantom models the trajectories lie in the regions $s > 0, r < 1$ while for Chaplygin gas model the trajectories lie in the regions $s < 0, r > 1$. In this paper we apply the statefinder diagnostic to the coupled phantom model. To begin with, we use another form of statefinder parameters in terms of the total energy density ρ and the total pressure p in the universe:

$$r = 1 + \frac{9(\rho + p) \dot{p}}{2\rho \dot{\rho}}, \quad s = \frac{(\rho + p) \dot{p}}{p \dot{\rho}}. \quad (16)$$

Since the total energy of the universe is conserved, we have $\dot{\rho} = -3H(\rho + p)$. Then making use of $\dot{\rho}_\phi = -3H(1 + \mathcal{W}_\phi^{eff})\rho_\phi$, we can get

$$r = 1 - \frac{3}{2} \mathcal{W}'_\phi \Omega_\phi + \frac{9}{2} \mathcal{W}_\phi (1 + \mathcal{W}_\phi^{eff}) \Omega_\phi, \quad (17)$$

$$s = 1 - \frac{\mathcal{W}'_\phi}{3\mathcal{W}_\phi} + \mathcal{W}_\phi^{eff}, \quad (18)$$

where $\mathcal{W}'_\phi = \frac{d\mathcal{W}_\phi}{dN}$. and the deceleration parameter is also given

$$q = \frac{1}{2} (1 + 3\mathcal{W}_\phi \Omega_\phi) \quad (19)$$

In the following we will discuss the statefinder for two scaling solutions with different conditions in Ref [18], and investigate how the interaction between phantom and dark matter influences the evolution of the universe. Firstly, we discuss the scaling solution B in the case of the interaction form (7), which exists for $x_B < 0$ (x_B is the initially velocity of the phantom field) and $0 < c \leq f(\frac{-\lambda - \sqrt{\lambda^2 + 12}}{2\sqrt{6}})$ ($f(x) \equiv x(2x + \sqrt{6}\lambda/3)(1 - \sqrt{6}x\lambda/3)$ is defined as a cubic function) and corresponds to a climbing-up phantom field. In this scenario, the universe ends with a big rip. In Fig. 1 we show the time evolution of the statefinder pairs $\{r, s\}$ and $\{r, q\}$ for the climbing-up scaling solution. The plot is for variable interval $N \in [-2, 20]$, and the selected evolution trajectories of $r(s)$ and $r(q)$ correspond to $\lambda = 1$, $c = 0, 0.1, 0.2$ and 0.3 respectively. $c = 0$ represents no interaction between phantom field and dark matter, $c = 0.1, 0.2$ and 0.3 represent the different transfer strength of interaction between DE and DM. We see clearly that the curve will pass through the LCDM fixed point when there is no coupling ($c = 0$) between phantom field and dark matter, while the distant from the curves to LCDM scenario is considerable when exists the interaction between phantom field and dark matter. The statefinder pair $\{r, s\}$ lies in the regions $s < 0, r > 1$, which is different from other quintessence and phantom model. In Fig. 2 we plot the evolution trajectories of the statefinder parameters versus redshift diagram of the climbing-up scaling solution with $x_0 < 0$. In the plots of the $-\ln(1+z) - r$ and $-\ln(1+z) - s$, we can see clearly that the interaction between phantom field and dark matter causes the big deviation between statefinder parameters and the LCDM scenario.

Next we discuss another scaling solution C in the case of the interaction form (7) in [18], which exists for $x_C > 0$ (x_C is also the initially velocity of the phantom field) and $0 < c \leq \min\{f(\frac{-\lambda + \sqrt{\lambda^2 + 6}}{\sqrt{6}}), f(\frac{-\lambda + \sqrt{\lambda^2 + 12}}{2\sqrt{6}})\}$, which

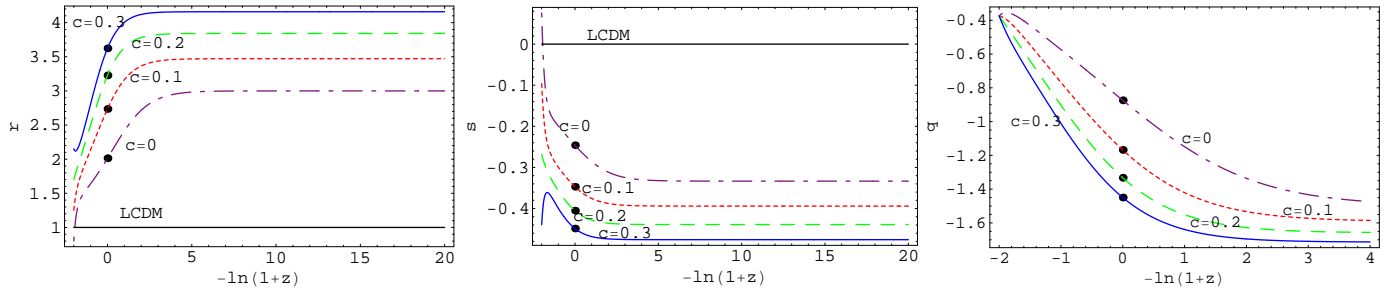


FIG. 2: The figures are the statefinder parameters versus redshift diagram of the climbing-up scaling solution with $x_0 < 0$. The left figure is $-\ln(1+z) - r$ diagram in the variable interval $N \in [-2, 20]$. The middle figure is $-\ln(1+z) - s$ diagram in the variable interval $N \in [-2, 20]$. The right figure is $-\ln(1+z) - q$ diagram in the variable interval $N \in [-2, 4]$. Selected curves for $\lambda = 1$, $c = 0, 0.1, 0.2$ and 0.3 respectively. Dots locate the current values of the statefinder parameters.

corresponds to a rolling-down phantom field where universe avoids the big rip. In Fig. 3 we show the time evolution of the statefinder pairs $\{r, s\}$ and $\{r, q\}$ for the rolling-down scaling solution. The plot is also for variable interval $N \in [-2, 20]$, and the corresponding parameters are also $\lambda = 1$, $c = 0, 0.1, 0.2$ and 0.3 respectively. We can see that the trajectories of this case will pass through LCDM fixed point. The statefinder pair $\{r, s\}$ lie in the region $s > 0$, $r < 1$ which is different from that in Fig. 1. In Fig. 4 we plot the evolution trajectories of the statefinder parameters versus redshift diagram of the rolling-down scaling solution with $x_0 > 0$. In the diagrams of the $-\ln(1+z) - r$ and $-\ln(1+z) - s$, we can see clearly that the interaction between phantom field and dark matter causes statefinder parameters to approach the LCDM scenario in the future. In Fig. 5, the evolution of the effective equation of state of the total cosmic fluid with different initial velocity have been shown. In the left figure, the phantom field initially climbs up, and the effective equation of state \mathcal{W}_{eff} tends to below -1 and realizes a transition from $\mathcal{W}_{eff} > -1$ to $\mathcal{W}_{eff} < -1$, thus the universe ends with big rip. In the right figure, the phantom field initially rolls down, the effective equation of state \mathcal{W}_{eff} tends to above -1 and realizes a transition from $\mathcal{W}_{eff} < -1$ to $\mathcal{W}_{eff} > -1$. In this case the universe avoids the big rip.

The scaling solutions B and C in [18] with different initially velocity of the phantom field cause the different evolution of the universe. We apply a statefinder analysis to this model, and contrast the scenario with coupling between phantom field and dark matter and the scenario without interaction between these two components. The difference can be found in Fig. 1–Fig. 4: (i) The region of the statefinder pair $\{r, s\}$ is different between Fig. 1 and Fig. 3, in Fig. 3 $s > 0$ and $r < 1$, while in Fig. 1 $s < 0$ and $r > 1$, which differs from the quintessence and phantom models. (ii) The influence of the interaction form is different in the evolution of the universe, which can be seen in the statefinder trajectories. In Fig. 2 we can see that the interaction form causes the big deviation between statefinder parameters and the LCDM scenario. In Fig. 4 the interaction causes statefinder parameters to approach the LCDM scenario in the future. In Fig. 5, the effective equation of state \mathcal{W}_{eff} realizes a transition from $\mathcal{W}_{eff} > -1$ to $\mathcal{W}_{eff} < -1$ and the universe ends with big rip if the phantom field initially climbs up. Contrarily, the effective equation of state transits from $\mathcal{W}_{eff} < -1$ to $\mathcal{W}_{eff} > -1$ and the universe avoids the big rip if the phantom field initially rolls down. So, through the statefinder diagnostic, we not only see the influence of the interaction form on the evolution of universe with different initial velocity, but also contrast the difference between the scenario with and without the interaction.

In summary, we study the statefinder parameters of the coupled phantom model. We analyze two cases of scaling solutions—the climbing-up scaling solution and rolling-down scaling solution, and contrast the difference between the scenario with and without the interaction. It is found that the evolving trajectories of these two scaling solutions in the $s - r$ and $q - r$ plane is quite different, and which is also different from the statefinder diagnostic of other dark energy models. We hope that the future high precision observation will be capable of determining these statefinder parameters and consequently shed light on the nature of dark energy.

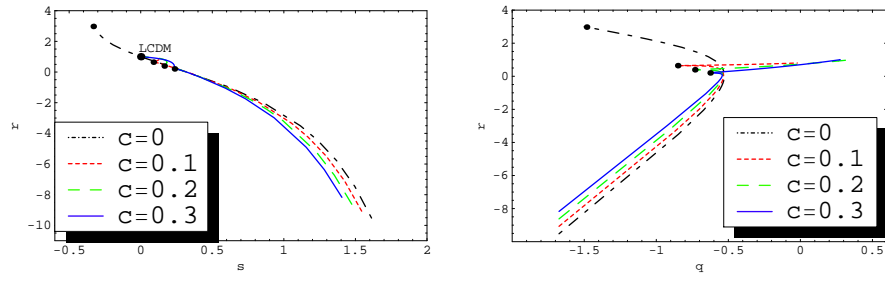


FIG. 3: The left figure is $s - r$ diagram of the rolling-down scaling solution with $x_0 > 0$. The right figure is $q - r$ diagram of the rolling-down scaling solution with $x_0 > 0$. The curves evolve in the variable interval $N \in [-2, 20]$. Selected curves for $\lambda = 1$, $c = 0, 0.1, 0.2$ and 0.3 respectively. Dots locate the current values of the statefinder parameters.

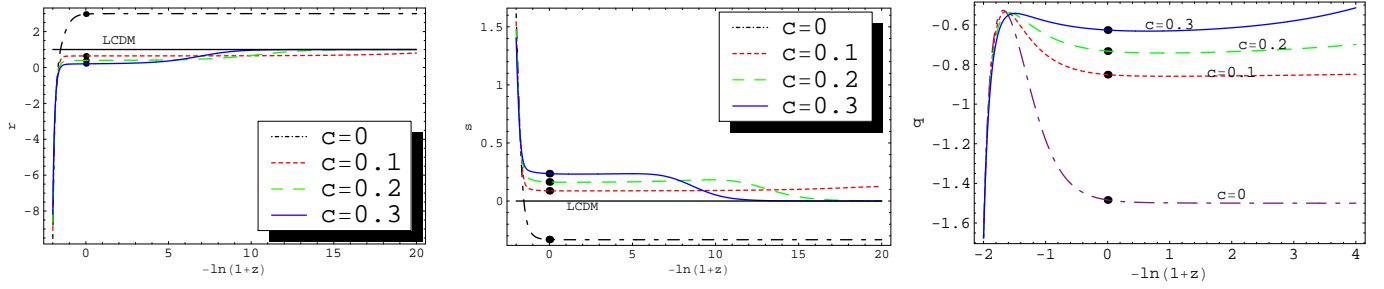


FIG. 4: The figures are the statefinder parameters versus redshift diagram of the rolling-down scaling solution with $x_0 > 0$. The left figure is $-\ln(1+z) - r$ diagram in the variable interval $N \in [-2, 20]$. The middle figure is $-\ln(1+z) - s$ diagram in the variable interval $N \in [-2, 20]$. The right figure is $-\ln(1+z) - q$ diagram in the variable interval $N \in [-2, 4]$. Selected curves for $\lambda = 1$, $c = 0, 0.1, 0.2$ and 0.3 respectively. Dots locate the current values of the statefinder parameters.

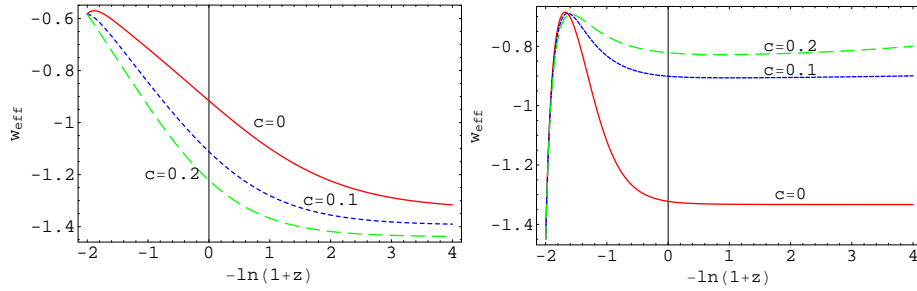


FIG. 5: The figures are the effective equation of state for the total cosmic fluid w_{eff} versus redshift. The left figure is $-\ln(1+z) - w_{eff}$ diagram of the climbing-up scaling solution with $x_0 < 0$. The right figure is $-\ln(1+z) - w_{eff}$ diagram of the rolling-down scaling solution with $x_0 > 0$. The curves evolve in the variable interval $N \in [-2, 4]$. Selected curves for $\lambda = 1$, $c = 0, 0.1$ and 0.2 respectively.

Acknowledgments

One of us (B. R. Chang) is grateful to Xin Zhang for helpful discussion. This work was supported by NSF (10573003), NSF (10647110), NBRP (2003CB716300) of P. R. China and DUT 893321.

-
- [1] A. G. Riess, et. al., *Astron. J.* **116**, 1009 (1998), astro-ph/9805201; S. Perlmutter, et. al., *Astrophys. J.* **517**, 565 (1999), astro-ph/9812133.
- [2] J. L. Tonry, et. al., *Astrophys. J.* **594**, 1 (2003), astro-ph/0305008; B. J. Barris, et. al., *Astrophys. J.* **602**, 571 (2004), astro-ph/0310843.
- [3] A. G. Riess et al., *Astrophys. J.* **607**, 665 (2004), astro-ph/0402512.
- [4] C. L. Bennett, et. al., *Astrophys. J. Suppl.* **148**, 1 (2003), astro-ph/0302207; D. N. Spergel, et. al., *Astrophys. J. Suppl.* **148**, 175 (2003), astro-ph/0302209.
- [5] M. Tegmark, et. al., *Phys. Rev. D* **69**, 103501 (2004), astro-ph/0310723; K. Abazajian, et. al., astro-ph/0410239; K. Abazajian, et. al., *Astron. J.* **128**, 502 (2004), astro-ph/0403325; K. Abazajian, et. al., *Astron. J.* **126**, 2081 (2003), astro-ph/0305492; E. Hawkins, et. al., *Mon. Not. Roy. Astron. Soc.* **346**, 78 (2003), astro-ph/0212375; L. Verde, et. al., *Mon. Not. Roy. Astron. Soc.* **335**, 432 (2002), astro-ph/0112161.
- [6] V. Sahni, A. Starobinsky, *Int. J. Mod. Phys. D* **9**, 373-444 (2000), astro-ph/9904398.
- [7] S. Weinberg, *Rev. Mod. Phys.* **61**, 1 (1989); S. M. Carroll, *Living Rev. Rel.* **4**, 1 (2001), astro-ph/0004075; P. J. E. Peebles and B. Ratra, *Rev. Mod. Phys.* **75**, 559 (2003), astro-ph/0207347; T. Padmanabhan, *Phys. Rept.* **380**, 235 (2003), hep-th/0212290.
- [8] B. Ratra and P. J. Peebles, *Phys. Rev. D* **37** 3406 (1988); R. R. Caldwell, R. Dave and P. J. Steinhardt, *Phys. Rev. Lett.* **80**, 1582 (1998); M.S. Turner, *Int. J. Mod. Phys. A* **17S1**, 180 (2002), astro-ph/0202008; V. Sahni, *Class.Quant.Grav.* **19**, 3435 (2002), astro-ph/0202076.
- [9] I. Zlatev, L. Wang, and P. J. Steinhardt, *Phys. Rev. Lett.* **82**, 896 (1999), astro-ph/9807002; P. J. Steinhardt, L. Wang, I. Zlatev, *Phys. Rev. D* **59**, 123504 (1999), astro-ph/9812313, X. Zhang, *Mod. Phys. Lett. A* **20**, 2575 (2005), astro-ph/0503072.
- [10] R. R. Caldwell, M. Kamionkowski, N. N. Weinberg, *Phys. Rev. Lett.* **91**, 071301 (2003), astro-ph/0302506; P. Singh, M. Sami, N. Dadhich, *Phys. Rev. D* **68**, 023522 (2003), hep-th/0305110; J. G. Hao, X. Z. Li, *Phys.Rev. D* **67**, 107303 (2003), gr-qc/0302100; Z. K. Guo, Y. S. Piao and Y. Z. Zhang, *Phys. Lett. B* **594**, 247-251 (2004), astro-ph/0404225; Elizalde E, Nojiri S and Odintsov S D, *Phys. Rev. D* **70**, 043539 (2004), hep-th/0405034; Mohseni Sadjadi H and Alimohammadi M, *Phys.Rev. D* **74**, 103007 (2006), gr-qc/0610080.
- [11] U. Alam, V. Sahni, T. D. Saini, A. A. Starobinsky, *Mon. Not. Roy. Astron. Soc.* **354**, 275 (2004), astro-ph/0311364; Y. Wang, P. Mukherjee, *Astrophys. J.* **606**, 654-663 (2004), astro-ph/0312192; S. Nesseris, L. Perivolaropoulos, *Phys. Rev. D* **70**, 043531 (2004), astro-ph/0401556; U. Alam, V. Sahni, A. A. Starobinsky, *JCAP* **0406**, 008 (2004), astro-ph/0403687; S. Hannestad, E. Mortsell, *JCAP* **0409**, 001 (2004), astro-ph/0407259, R. A. Knop et al., *Astrophys. J.* **598**, 102 (2003), astro-ph/0309368.
- [12] R. R. Caldwell, *Phys. Lett. B* **545**, 23 (2002), astro-ph/9908168.
- [13] A. A. Starobinsky, *Grav. Cosmol.* **6**, 157-163 (2000), astro-ph/9912054.
- [14] M. Sami and A. Toporensky, *Mod. Phys. Lett. A* **19**, 1509 (2004); P. F. Gonzalez-Diaz, *Phys. Lett. B* **586**, 1 (2004); L. P. Chimento and R. Lazkoz, gr-qc/0405020; R. R. Caldwell, M. Kamionkowski, and N. N. Weinberg, *Phys. Rev. Lett.* **91**, 071301 (2003), astro-ph/0302506; Nojiri S, Odintsov S D and Tsujikawa S, *Phys. Rev. D* **71**, 063004 (2005), hep-th/0501025.
- [15] S. M. Carroll, M. Hoffman and M. Trodden, *Phys. Rev. D* **68**, 023509 (2003); P. Singh, M. Sami and N. Dadhich, *Phys. Rev. D* **68**, 023522 (2003); Z. K. Guo, Y. S. Piao and Y. Z. Zhang, *Phys. Lett. B* **594**, 247 (2004); I. Y. Arefeva, A. S. Koshelev and S. Y. Vernov, astro-ph/0412619.
- [16] Z. K. Guo, Y. S. Piao, X. M. Zhang, Y. Z. Zhang, *Phys. Lett. B* **608**, 177-182 (2005), astro-ph/0410654; J. G. Hao, X. Z. Li, *Phys. Rev. D* **70**, 043529 (2004), astro-ph/0309746.
- [17] Z. K. Guo, Y.Z. Zhang, *Phys.Rev. D* **71**, 023501 (2005), astro-ph/0411524.
- [18] Z. K. Guo, R. G. Cai and Y. Z. Zhang, *JCAP* **0505**, 002 (2005), astro-ph/0412624.
- [19] Z. K. Guo, Y. S. Piao, R. C. Cai and Y. Z. Zhang, *Phys. Lett. B* **576**, 12-17 (2003), hep-th/0306245; B. R. Chang, H. Y. Liu and L. X. Xu, *Mod. Phys. Lett. A* **20**, (2005) 923, astro-ph/0405084; L. X. Xu, H. Y. Liu, *Int. J. Mod. Phys. D* **14**, 1947-1957 (2005), astro-ph/0507250; H. Y. Liu, H. Y. Liu, B. R. Chang and L. X. Xu, *Mod. Phys. Lett. A* **20**, (2005) 1973-1982, gr-qc/0504021.
- [20] W. Zimdahl and D. Pavon, *Gen. Rel. Grav.* **36**, (2004) 1483.
- [21] V. Sahni, T. D. Saini, A. A. Starobinsky and U. Alam, *JETP Lett.* **77**, 201 (2003), astro-ph/0201498.
- [22] U. Alam, V. Sahni, T. D. Saini and A. A. Starobinsky, *Mon. Not. Roy. ast. Soc.* **344**, (2003) 1057, astro-ph/0303009; V. Gorini, A. Kamenshchik and U. Moschella, *Phys. Rev. D* **67**, (2003) 063509, astro-ph/0209395; X. Zhang, *Phys. Lett. B* **611**, 1 (2005), astro-ph/0503075; X. Zhang, *Int. J. Mod. Phys. D* **14**, 1597 (2005), astro-ph/0504586; P. X. Wu and H. W. Yu, *Int. J. Mod. Phys. D* **14**, 1873-1882 (2005), gr-qc/0509036, X. Zhang, F. Q. Wu, J. F. Zhang, *JCAP* **0601**, 003 (2006), astro-ph/0411221; Setare M R, Zhang J F, Zhang X, gr-qc/0611084.